29th International Cosmic Ray Conference Pune (2005) **6**, 209–212

A detailed study on nuclear composition of primary cosmic rays around the knee with GRAPES-3

H. Tanaka[b], S.K. Gupta[a], Y. Hayashi[b], N. Ito[b], A. Jain[a], A.V. John[a], S. Karthikeyan[a], S. Kawakami[b], H. Kojima[c], K. Matsumoto[b], Y. Matsumoto[b], T. Matsuyama[b], D.K. Mohanty[a], P.K. Mohanty[a], S.D. Morris[a], T. Nonaka[b], T. Okuda[b], A. Oshima[b], B.S. Rao[a], K.C. Ravindran[a], K. Sivaprasad[a], B.V. Sreekantan[a], S.C. Tonwar[a], K. Viswanathan[a] and T. Yoshikoshi[b]

(a) Tata Institute of Fundamental Research, Homi Bhabha Road, Mumbai 400 005, India
(b) Graduate School of Science, Osaka City University, Osaka 558-8585, Japan
(c) Nagoya Women's University, Nagoya 467-8610, Japan
Presenter: H. Tanaka (tanaka@alpha.sci.osaka-cu.ac.jp), jap-tanaka-H-abs1-he12-oral

GRAPES-3 is a high-density air shower array with large area muon detectors. The energy spectra of various nuclei (H, He, N, Al and Fe) and their mean mass have been obtained through a combination of observations on electrons and muons. The mean mass number gradually increases through the *knee* region. These results show dependence on the hadronic interaction models of EAS Monte Carlo. Two models, QGSJET and SIBYLL, were investigated and their results were compared with those from direct measurements. Predictions of SIBYLL agree with JACEE results, but some discrepancy is seen between QGSJET and JACEE. Some models proposed in literature to explain the occurrence of the *knee* are used to compare them with our results.

1. Introduction

Cosmic ray energy spectrum displays a *knee* around 3×10^{15} eV, where the index of power law spectrum changes from ~ -2.7 to ~ -3.1. The *knee* region is expected to provide information on the origin of cosmic rays. It is hoped that accurate measurement of cosmic ray spectra and nuclear composition around the *knee* would help promote a better understanding of cosmic ray origin.

The *knee* region is difficult to access with direct measurement at the top of atmosphere such as balloon and satellite based experiments due to low flux of cosmic rays which requires large area and heavy detectors are flown. Therefore indirect measurement with air shower observation is the only practical way to reach higher energies.

Monte Carlo simulation is used to reconstruct the shower in the atmosphere and estimate properties of primary particle from observed data. This kind of analysis is, however, limited by the reliability of simulation models used because of extrapolations of high energy interaction models based on accelerator data. Here we have used a few models and have studied the dispersion in their predictions.

2. Experimental Methods

The GRAPES-3 air shower array is located at Ooty in southern India at an altitude of 2,200 m above sea level. It consists of nearly 300 scintillation detectors to measure the electron component and about 3700 proportional counters to detect muons in showers. [1][2]

CORSIKA (v6.02)[3] EAS MC code is used for the simulation of observations. The EAS simulations have the uncertainties of hadronic interactions due to extrapolation of the measurements to the energy of EAS. COR-

SIKA incorporates several hadronic interaction models and here we use the following two, QGSJET (2001) model and SIBYLL (2.1) model which have been developed for EAS simulations.

A total of 6×10^8 showers observed during two years of run in 2000 and 2001 (~ 560 days) have been analyzed. Size of each shower is estimated from lateral distribution of particles with a Maximum Likelihood Method fit to NKG function. Here the free parameters are shower core location $\mathbf{R}$, shower size N_e and age s.

Tracks of muons are reconstructed using tracking muon detectors to agree with shower direction. It helps to reduce the background of muons. Reconstructed showers are selected to be within a fiducial area and 80 m away from muon detectors, which is shown as yellow (or gray) area in Figure 1, to reject distant showers outside the array and to prevent saturation of muon detectors.

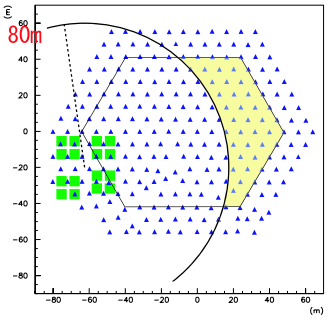

Figure 1. Shower detectors (plastic scintillator 1 m^2 each) and muon detectors (total 560 m^2) are shown with ▲ and ■ respectively. Here, core location shown in yellow (or gray) area is located inside the array but $\geq$ 80 m away from muon detectors.

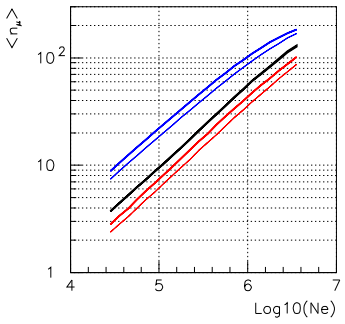

Figure 2. Relation between shower size and average number of muons. Black line shows the results from observation. Red and blue lines show MC results for proton and iron primaries. Dependence on the hadronic interaction models is represented by QGSJET (fat lines) and SIBYLL (fine lines).

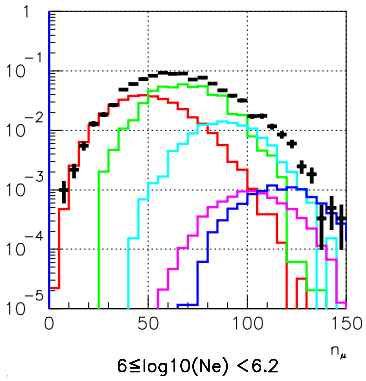

Figure 3. Muon multiplicity distributions classified by shower size. Observations are shown in black. MC (QGSJET) results for proton, helium, nitrogen, aluminum and iron are shown in red, green, light blue, violet and blue respectively. MC distributions are fitted to observations to estimate relative abundance for each.

In Figure 2, average number of detected muons is shown for a given shower size. CORSIKA MC results are also shown for proton and iron nuclei. The $N_e - N_\mu$ relation features the primary nuclear composition. Results bases on hadronic interaction models, QGSJET and SIBYLL, are presented here.

The energy spectrum of each component can be extracted from the shapes of muon multiplicity distributions. Figure 3 shows the muon multiplicity distributions from observation and MC's after fitting them to the observations to estimate relative abundance for each component. Here, the ratio of abundance of aluminum to iron is fixed to 0.8, because it is difficult to separate them. This value was decided from extrapolation of low energy observations by RUNJOB. The relations between shower size and primary energy are calculated by MC for each mass groups and the primary energies are converted from shower size as explained below. The MC is carried out using $E^{-2.7}$ spectrum and then the MC showers are subjected to same cuts as observational data. They are binned according to shower size and then the mean energy $< \log E >$ for each bin is calculated. [4]

3. Results and Conclusions

The energy spectra and mean mass values derived from GRAPES-3 data are shown and compared with other observations in Figure 4, 5, 6 and 7.

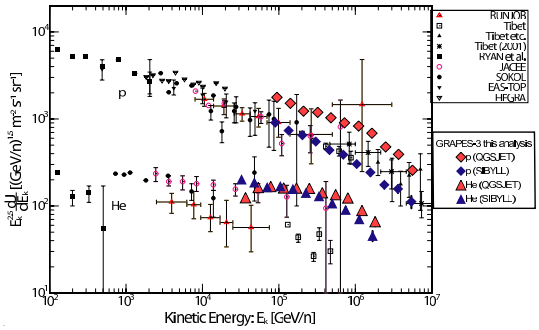

Figure 4. A comparison proton and helium energy spectra with other observations, RUNJOB, Tibet, EAS-TOP etc. from Kobayakawa et al.[5]

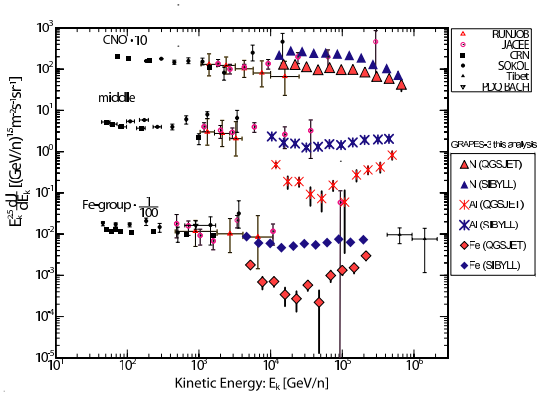

Figure 5. A comparison of energy spectra of CNO, medium heavy and iron groups with other observations. The flux of CNO and Fe-groups is multiplied by 10 and $1/100$, respectively. [5]

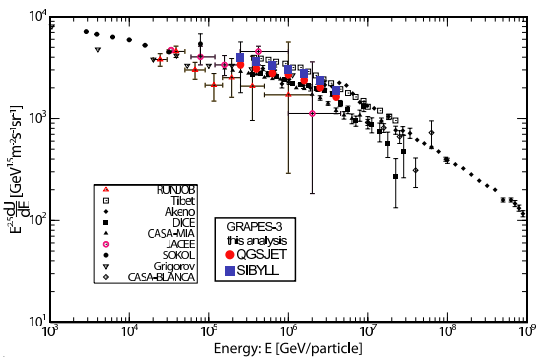

Figure 6. A comparison of all-particle energy spectra. GRAPES-3 compared with RUNJOB, Tibet, Akeno, CASA-DICE, CASA-MIA, CASA-BLANCA etc. [5]

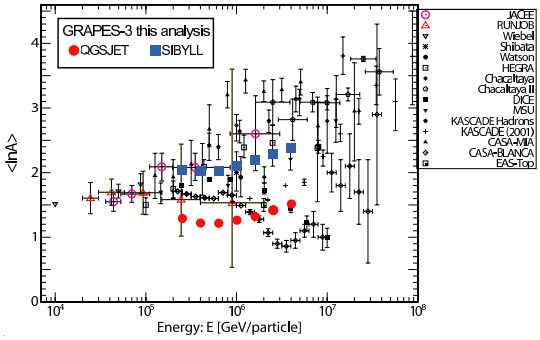

Figure 7. A comparison of mean mass ($\langle \ln A \rangle$) for GRAPES-3 with JACEE, RUNJOB, CASA-DICE, CASA-MIA, CASA-BLANCA, EAS-TOP, KASCADE, Chacaltaya etc. [5]

In Figure 6, the effect of interaction models is relatively small and flux from QGSJET is only 20% higher than SIBYLL. No disagreement with other experiments is found for both models with all-particle spectra. However, there are significant differences in the flux for each component. In Figure 4 and 5, QGSJET flux is higher for proton, and SIBYLL is higher in heavier component.

Since direct observations are good checks on the interaction model, a comparison of direct results from JACEE

with QGSJET and SIBYLL shows good agreement with SIBYLL and some disagreement with QGSJET results.

A comparison of the mean masses is shown in Figure 7. SIBYLL has $0.7 \sim 0.8$ larger $\langle \ln A \rangle$ than QGSJET. Both have tendency to increase $\langle \ln A \rangle$ above 10^6 GeV. Here, SIBYLL has good agreement with direct measurements, too.

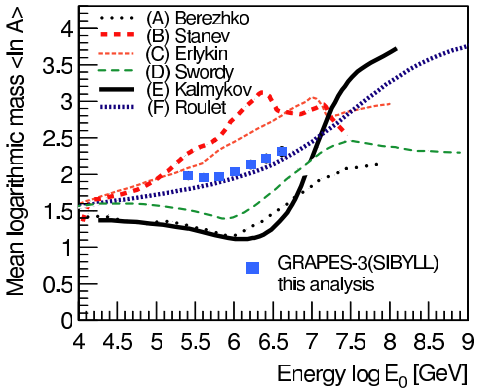

Figure 8. A comparison of GRAPES-3 results with SIBYLL using six models of the *knee* from J.R. Hörandel[6].

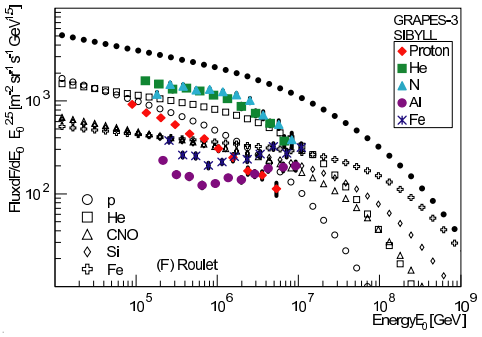

Figure 9. Diffusion and drift (F) *knee* model by E. Roulet[7] and GRAPES-3 results using SIBYLL.

Some models are suggested to reproduce *knee* in the energy spectrum. In Figure 8, plots of mean mass number which are expected from various *knee* models are shown[6] and results from SIBYLL, which is one of the most reliable model of hadronic interactions are also shown. Results from the following models of *knee*, (A) Acceleration in supernova remnants, (B) Acceleration by supernova shocks, (C) The single-source model, (D) The minimum-pathlength model, (E) Drift in the global regular magnetic field of the Galaxy and (F) Diffusion and drift are shown in Figure 8. (A) $\sim$ (C) expect *knee* appears due to acceleration mechanisms, (D) $\sim$ (F) it is due to propagation and leakage. In these, similar results are obtained from "(F) Diffusion and drift" model by comparison of energy spectrum for each mass component.

In Figure 9, CNO flux is $1/3$ smaller than SIBYLL, though it has good agreement in proton and helium spectra. In the above, there is no model which agrees with our results completely, although "Diffusion and drift" model has almost same results as our data.

References

[1] S.K. Gupta et al. *Nucl. Instr. & Meth. A*, 540, 311 (2005).
[2] Y. Hayashi et al. *Nucl. Instr. & Meth. A* 545, 643 (2005).
[3] D. Heck et al. *Forschungszentrum Karlsruhe*, FZKA 6019 (1998).
[4] H. Tanaka et al. *Proc. 28th ICRC*, 1, 155, Tsukuba (2003).
[5] K. Kobayakawa et al. *Phys. Rev. D*, 66(8), 083004 (2002).
[6] J.R. Hörandel. *Astropart. Phys.*, 21, 241 (2004).
[7] E. Roulet. *Int. J. Mod. Phys. A*, 19(7), 1133 (2004).